Coherent growth of oxide films on a cleaved layered metal oxide substrate

Prahald Siwakoti, Hangwen Guo, Zhen Wang, Yimei Zhu, Rosalba Fittipaldi, Antonio Vecchione, Y. Wang, Zhiqiang Mao, and Jiandi Zhang

Phys. Rev. Materials **2**, 104407 — Published 18 October 2018

DOI: 10.1103/PhysRevMaterials.2.104407

Coherent growth of oxide films on a cleaved layered metal oxide substrate

Prahald Siwakoti[1], Hangwen Guo[1], Zhen Wang[1,2], Yimei Zhu[2], Rosalba Fittipaldi[3], Antonio Vecchione[3], Y. Wang [4] Zhiqiang Mao[4], and Jiandi Zhang[1]

[1]*Department of Physics and Astronomy, Louisiana State University, Baton Rouge, LA 70803*

[2]*Department of Energy Science and Technology, Brookhaven National Laboratory, Upton, New York 11973, USA*

[3]*CNR-SPIN Unità di Salerno and Dipartimento di Fisica "E.R. Caianiello" Università di Salerno, I-84084 Fisciano, Salerno, Italy*

[4]*Department of Physics and Engineering Physics, Tulane University, New Orleans, Louisiana 70118, USA*

Abstract

Understanding oxide interface-induced effects require controlled epitaxial growth of films on well-defined substrate surfaces. While conventional film growth on *ex-situ* prepared substrates has proven to be a successful route, the choices of appropriate substrates with atomically defined surfaces are limited. Here, by depositing $La_{2/3}Sr_{1/3}MnO_3$ on Sr_2RuO_4 (001), we present an alternative method of growing oxide thin films on *in-situ* cleaved surfaces of layered-structured substrates. Cleaving Sr_2RuO_4 at low temperature in ultra-high vacuum exposes an atomically flat, solely SrO-terminated surface with up to micrometer scale terraces. The deposition of $La_{2/3}Sr_{1/3}MnO_3$ spontaneously diminishes the surface RuO_6 in-plane rotational distortion of the substrate and results in a cubic-like perovskite film structure with (La/Sr)-O layer termination. The interface is atomically sharp without obvious deviation of lattice spacing and chemical valence, except in the first unit cell where Ru-Mn intermixing is observed. These results demonstrate that film growth on a cleaved substrate can be an alternative route to obtain well-defined interfaces and in addition increase the availability of substrates for future oxide films.

INTRODUCTION

The physical properties of thin film materials can be significantly influenced by the epitaxial strain induced by varieties of substrates. The method of strain engineering in complex oxide thin films has been a subject of interest for decades [1–5]. The choice of substrate affects different aspects of the film growth, from the feasibility of growth to the quality of the thin films produced. The established procedure in the community is to obtain commercially available substrates such as widely used $SrTiO_3$ that are mechanically cut along a crystallographic direction and polished. These as-received crystals are not chemically singly-terminated in most cases and must go through substrate-specific procedures like chemical etching, annealing, etc. to get the desired termination layer. Moreover, the choices of commercial substrates for transition metal oxide (TMO) thin film growth are largely limited by chemical and structural compatibility and lattice mismatch.

To overcome these barriers, we take an alternative approach that uses cleavable layered crystals. Many layered crystals cleave naturally to provide a surface with a specific terminating layer. In this work, we present the epitaxial layer−by-layer growth of high-quality thin films on a layered single crystal with an atomically defined interface. We choose single crystals of Sr_2RuO_4 (SRO214) as our substrate and grow $La_{2/3}\,Sr_{1/3}MnO_3$ (LSMO) thin films on them. LSMO in its bulk structure has a rhombohedral space group symmetry with lattice constant a = 3.878 Å, whereas SRO214 in bulk exhibits a body-centered tetragonal space group (*I4/mmm*) symmetry with lattice parameters a = 3.873 Å and c = 12.74 Å. The lattice mismatch between these systems is ~ -0.1%. This near perfect lattice match is important to avoid any strain-induced effects on the system. An atomically flat SrO-terminated surface is naturally formed after *in-situ* cleaving,

which allows for a sharp interface to be achieved after LSMO thin film growth. This approach can be easily applied to numerous layered compounds, which not only expands the choice of substrates but also paves the way to study a variety of substrate – thin film interactions.

More importantly, the interface of LSMO/SRO214 heterostructures can be a good candidate for the study of the proximity effect between ferromagnetic (FM) metals and unconventional superconductors. The superconductivity in SRO214 is distinct due to its *p*-wave nature with spin-triplet pairing and a broken time reversal symmetry [6]. LSMO is a ferromagnetic half-metal with a high curie temperature, showing colossal magnetoresistance and near 100% spin polarization [7,8]. The LSMO/SRO214 heterostructure can serve as a prototype system to study long-range spin-polarized supercurrent [9–15]. Both charge and spin supercurrent are expected to be generated across the FM/Triplet spin Superconductor (TSC) interface [16,17] even in the absence of interfacial magnetic inhomogeneity. The quality of the interface is essential in these types of experiments. The atomically sharp interface we fabricated can help minimize the undesired impurity scattering that can cause coherency loss in supercurrents.

I. EXPERIMENTAL METHODS

The SRO214 single crystals employed as the substrate were grown by using the floating zone technique [18,19]. They were cleaved *in-situ* at a temperature of 77 K and base pressure of 1×10^{-9} Torr. An Al rod was glued onto a crystal substrate using silver epoxy. The substrate with the Al was then transferred into the cleaving chamber and cooled down to liquid nitrogen temperature. The crystal was cleaved by knocking off the Al rod to obtain the SRO214 (001) surface and then transferred to the main characterization chamber with a base pressure of 2×10^{-10} Torr. The cleaved surfaces obtained were characterized using low energy electron diffraction (LEED) and scanning tunneling microscopy (STM). The LEED analysis on the single crystal

substrate was performed at room temperature. STM images were taken using an *in-situ* STM. SRO214 single crystals of dimensions 5 mm × 3 mm × 0.5 mm were used as substrates to grow LSMO thin films using Pulsed Laser Deposition (PLD). A stoichiometric LSMO target was illuminated with a KrF excimer laser (λ = 248 nm) at a repetition rate of 10 Hz and a laser energy of 120 mJ. The oxygen partial pressure of 80 mTorr, which is the total pressure of the chamber as read from the pressure gauge, was obtained with a mixture of 99% O_2 and 1% O_3 and maintained during growth while the substrate temperature was fixed at 700 °C. Thin film growth was monitored using Reflection High Energy Electron Diffraction (RHEED) oscillations. The chemical composition of LSMO films was studied using angle resolved X-ray photoelectron spectroscopy (ARXPS). A monochromated Al Kα x-ray source and a PHOIBOS 150 energy analyzer, both from SPECS, were used to measure the core level spectra of Sr 3d and Mn 2p. The energy analyzer was calibrated with the core level of single crystalline gold (Au $4f_{7/2}$ peak).

Cross sectional Scanning Transmission Electron Microscopy (STEM) samples, with thicknesses of about 50 nm, were prepared using Focused Ion Beam (FIB) with Ga^+ ions followed by Nano milling with Ar^+ ions to remove the surface damage on the samples. Structural and chemical information, as well as evolution, across the LSMO/SRO214 interface, was studied using atomically resolved STEM imaging and electron energy-loss spectroscopy (EELS). The STEM/EELS experiments were performed on the 200 kV JEOL ARM electron microscope at Brookhaven National Laboratory equipped with double aberration correctors and a dual-energy-loss spectrometer. The STEM images were collected with a condense aperture (30 μm) of 21 mrad and a collection angle of 67 - 375 mrad for high-angle annular dark field (HAADF) and 11 – 23 mrad for annular bright-field (ABF) images. Scanning EELS spectra were obtained across the whole film with a step size of 0.13 Å, a convergence semi-angle of 20 mrad, and a collection

semi-angle of 88 mrad. Dual EELS mode was used to remove the intrinsic energy shifts of the electron beam introduced in the EELS scanning process. The EELS spectra were background subtracted with a power-law function, and multiple scattering was removed by a Fourier deconvolution method.

II. RESULTS AND DISCUSSIONS

A ball model schematically showing the arrangement of atoms in the LSMO film grown on SRO214 is presented in Fig. 1(a), based on the tetragonal structure of SRO214 and cubic structure of LSMO. Fig. 1(b) shows the real-time RHEED signal by monitoring diffraction spot intensity during LSMO thin film growth. LSMO thin films exhibit an excellent 2D layer-by-layer growth. We note that the reduction of RHEED intensity compared to SRO214 substrate can be due to the enhanced electron scattering from a mixed La/Sr layer. Before the deposition, the surface morphology and lattice structure of the substrate were characterized *in-situ* by LEED and STM.

STM topography images of a freshly cleaved surface, as shown in Fig 2(a), reveal that cleaving at low temperature and high vacuum exposes large flat terraces. The formation of such large flat terraces decreases the step density at the surface which can be advantageous for future electronic measurements of the FM/TSC heterostructures because fewer steps allows for less leakage currents from conducting substrates. The step heights are found to be integral multiples of half the unit-cell length in the c-direction (6.4Å) as can be seen in the line profile graph in Fig. 2(b). This is indicative of the fact that the cleaving occurs between two weakly bonded SrO layers. The SrO-layer termination of the substrate surface is also confirmed by the surface structure determined by LEED I(V) analysis [20]. Fig. 2(c) shows the LEED diffraction image of the surface of a freshly cleaved SRO214. The diffraction pattern consists of both integer spots and

fractional spots with two orthogonal glide lines, showing a ($\sqrt{2} \times \sqrt{2}$) R45° reconstructed unit cell, indicating a surface reconstruction in agreement with previous studies. At the surface, the Σ_3 zone boundary soft-phonon mode in the bulk freezes into a static lattice distortion associated with an in-plane rotation of the RuO_6 in the top octahedral layer [20].

To understand if annealing the substrate at high temperatures during growth affects the structure of the surface, we performed LEED experiments on annealed substrate samples to 700 °C in the presence of O_2 to mimic the growth condition. The fractional spots, corresponding to a ($\sqrt{2} \times \sqrt{2}$) R45° reconstructed unit cell, are still observed, as shown in Fig. 2 (d), but we observe an increase in the background and a reduction in intensity of the fractional spots. Such a reduction can be mainly due to the disordering effect by generating vacancies at the surface. Interestingly, when depositing the LSMO film, the LEED image from the surface exhibits only integer spots with no fractional ones, corresponding to the 1×1 LEED pattern of the unreconstructed surface. As an example, Fig. 2(e) displays the LEED pattern of a 10 unit – cell (u.c.) LSMO thin film grown on SRO214. This 1×1 surface structure is observed beginning at the first unit cell of film coverage and stays regardless the film thickness. This indicates that the rotational distortion of the RuO_6 octahedra at the substrate surface is diminished as the film growth begins. Therefore, we believe the surface layer of SRO214 restores itself back to a non-distorted tetragonal structure when the interface is formed even though further study of the interface structure is needed.

To probe the possible variation of stoichiometry at the surface of the LSMO thin films, the core level spectra were measured by ARXPS. The depth profile of chemical components can be extracted from the ARXPS data by knowing their relative photoionization cross-sections and mean free paths [21]. Figure 2(f) shows the core level peaks observed for Mn 2p and Sr 3d respectively. The spectra taken at a large collection angle θ are more surface sensitive owing to

shorter probing depth than at normal emission. The Sr 3d peak shape changes with an increase in surface sensitivity. We have calculated the intensity ratio of Sr 3d peaks to Mn 2p peaks at normal emission $\theta = 0^o$ and compared it to the value of the ratio obtained at $\theta = 60^o$, as shown in the inset in Fig. 2 (f). The increase in this ratio at $\theta = 60^o$ relative to that at normal emission suggests that the surface of the film is strontium rich, and it is therefore likely that the surface is terminated with a SrO layer. Furthermore, the increment of the ratio with increasing θ also suggests Sr - segregation at the surface of LSMO. This result is consistent with LSMO films grown on other commercial substrates [22–24]. The strontium segregation to the surface has been found to be strongly affected the oxygen environment and temperature during growth [25,26]. Since the La/Sr – O layer in LSMO is a polar surface, Sr segregating to the surface would compensate for the charge imbalance because SrO is non-polar. Strontium segregation in these films has been found to behave exponentially.

It is known that the change in Sr and La cation ratio in the film indicates change in the proportion of Mn^{3+} and Mn^{4+} ions at different atomic sites. The proportion of Mn valence is crucial for the double exchange mechanism that leads to ferromagnetism in the LSMO [27,28]. While the line shape and peak position of Mn 2p peaks in XPS are not very sensitive to the Mn chemical valence, the position of shakeup satellites can be used to identify the Mn valence [29]. The shakeup satellite observed is broad and has a binding energy about 10 eV higher than the $2p_{1/2}$ peak. The Mn 2p peaks taken at different collection angle are very similar. Also, Mn-3s doublet splitting has been known to increase with decreasing Sr content. However, we do not observe any change in Mn 3s splitting with surface sensitivity, suggesting no sizeable change in Mn valence at the surface. This is also in agreement with STEM EELS results presented later.

Knowing the overall quality of the thin film, an important next question to address is the quality of the interface. This is particularly important for the study of many electronic and magnetic interactions driven by interfacial proximity effects. We have examined the interface by employing atomic resolved STEM. In Fig. 3(a) a large scale HAADF-STEM image for an LSMO/SRO214 film taken along the [100] direction shows an atomically well-defined and coherent interface without obvious dislocations. High magnification HAADF- and ABF-STEM images at the interface are presented in Fig. 3(b). Oxygen can clearly be seen in the ABF image, because the bright field detectors are sensitive to light elements. The position of the interface in these images, as indicated by a yellow dotted line, can be determined based on the intensity profile of the HAADF image plotted at the bottom of Fig. 3(b). The column intensity in the HAADF image is proportional to atomic number (Z), and the intensity decreases as we move from Ru to La/Sr, La/Sr to Sr, and Sr to Mn columns. Near the interface, the intensity of the first layer of Mn in the film side as well as the first layer of Sr on the substrate side has increased. This indicates intermixture with heavier elements on the both sides. The termination layer of the substrate is clearly SrO, thus confirming that cleaving happens at the two weakly bonded SrO layers without breaking the RuO_6 octahedra.

To evaluate the possible variation in lattice structure across the interface, we extract the *c*-axis lattice parameters in the atomic layer-by-layer steps near the interface of the substrate and film as shown in Fig. 3(c). On the SRO214 side, the measured *c*-axis lattice parameter is identical to that in the bulk of SRO214, except for the interface layer where RuO_6 is elongated by ~0.1 Å along the [001] direction. The *c*-axis lattice spacing of the film, however, is slightly larger than the bulk value. Notably, the first MnO_6 octahedron layer has an out-of-the-plane lattice expansion by more than 0.1 Å. The observation of this tetragonal distortion of the film in the absence of lattice

mismatch with the substrate is surprising and needs further exploration. One possibility is that LSMO in this epitaxial film becomes tetragonal by diminishing the rhombohedral distortion existing in bulk LSMO.

To characterize the nature of intermixing at the interface, we performed a detailed EELS study. Chemical intermixing is commonly observed in oxide thin films and tends to be unavoidable. Figure 3(d) shows the layer-by-layer averaged elemental profiles, extracted from the EELS spectra by integrating the signal of La-M, Ru-M, Sr-L, and Mn-L edges, superimposed onto the corresponding atomic sites in the HAADF images. Since the intensity of Mn in the first layer is significantly smaller and Ru does not drop down to zero in the first layer of MnO_2 at the interface, Ru-Mn intermixing may occur in the first unit-cell at the interface. The intensity of Sr in the first La/Sr-O layer in the film is larger than the bulk stoichiometric value of 33% and is accompanied by a decrease in La intensity in the same layer. This suggests that La/Sr intermixture also happens in the first unit cell at the interface.

We further examined the fine structure of O K and Mn L edge excitations in EELS spectra, as displayed in Fig. 4(a), to gain insight into the electronic properties at the interface. The first peak labelled ‘a’, commonly referred as a pre-peak, has a strong contribution from the Mn 3d e_g band. This peak is sensitive to bonding features of the octahedron [30]. The second peak labelled ‘b’, however, is commonly attributed to the hybridization of the O 2p with La 5d and/or Sr 3d bands [31]. No notable change in both these peaks is observed across the interface. This tells us that the nature of the chemical bonding of the oxygen do not change in going from the substrate to the film. The energy separation between the peaks ‘a’ and ‘b’ in the O-K edges is an accurate method to quantify the Mn oxidation states [31]. Figure 4(b) shows that, in the LSMO film, the peak energy separation does not change, suggesting a uniform oxidation state in the film.

Mn L edges are the results of excitations of Mn 2p electrons to the unoccupied d states above the Fermi energy. Mn L edges consist of two white lines L_3 and L_2 arising due to transitions from $2p_{3/2}$ and $2p_{1/2}$ core states to 3d unoccupied states. The ratio of the intensities of the L_3 and L_2 lines is also characteristic of the manganese oxidation states. Using EELS spectra collected from bulk LSMO samples as reference, the oxidation states of Mn ions can be determined from the Mn $L_{2,3}$ ratio and is shown in Fig. 4(c). The value of ~ (3.31 ± 0.08) measured for the LSMO film is very close to what one would expect for bulk LSMO. The Mn valence appear to stay uniform throughout the film up to the surface, which does not account for the Sr segregated to the surface. The amount of Sr segregation is not large enough to produce a significant change in stoichiometry at the surface to be reflected in the L_{23} ratio. However, for the Mn doped into the top RuO_2 layer on the substrate side, the Mn $L_{2,3}$ ratio does increase, suggesting a lower chemical valence of Mn. This is unusual since Mn would be expected to increase its valence when it replaces the Ru^{4+} ion in SRO214. The possible existence of high density of oxygen vacancies at the interface is a feasible explanation for this behavior, but further study is required.

III. CONCLUSION

We have successfully grown high quality LSMO thin films on SRO214 single crystal substrates with perovskite (113/214) stacking and a sharp interface. Comprehensive characterization with LEED, RHEED, STM and ARXPS confirms the successful growth with correct stoichiometry and ordered film surface. The surface reconstruction of the SRO214 substrate associated with the top layer RuO_6 rotational distortion disappears with the deposition of LSMO and results in a cubic-like perovskite film structure with (La/Sr)O layer termination. STEM results reveal a high quality, atomically sharp interface with single-layer minimal chemical intermixing and minimal lattice spacing deviation.

The presented growth approach can lead to further exploration of interface-driven proximity effects between ferromagnetic (FM) half metals and triplet-spin superconductors (TSC). Owing to the well-defined interface, our LSMO/SRO214 heterostructure can be a good candidate to realize proximity effects and long-range spin-transport in FM/TSC devices. The atomically sharp interface we fabricated can help minimize the undesired impurity scattering and gain insight into the intrinsic properties therein. Finally, our approach is not constrained in the framework of TSC and FM metal interfaces. The successful demonstration of coherent growth enables a new pathway to expand the choice of substrate greatly. Many Ruddlesden-Popper (R-P) layered compounds beyond the typical commercially available options can be utilized as substrates for thin film growth. We expect proximity effects originated from these numerous exotic substrates can lead to new discovery of novel interface phenomena.

Acknowledgments: We would like to thank Dr. M. Saghayezhian for help with experiments. This work is primarily supported by the US NSF under Grant No. DMR 1608865. The electronic microscopic work done at Brookhaven National Laboratory is sponsored by the US DOE Basic Energy Sciences, Materials Sciences and Engineering Division under Contract DE-AC02-98CH10886. Z.W. and H.G. were supported by the U.S. DOE under Grant No. DOE DE-SC0002136. The single crystal growth effort at Tulane was supported by the U.S. Department of Energy under EPSCoR Grant No. DE-SC0012432 with additional support from the Louisiana Board of Regents.

References:

[1] J. Wang, J. B. Neaton, H. Zheng, V. Nagarajan, S. B. Ogale, B. Liu, D. Viehland, V.

Vaithyanathan, D. G. Schlom, U. V Waghmare, N. A. Spaldin, K. M. Rabe, M. Wuttig, and R. Ramesh, Science **299**, 1719 (2003).

[2] D. G. Schlom, L.-Q. Chen, C.-B. Eom, K. M. Rabe, S. K. Streiffer, and J.-M. Triscone, Annu. Rev. Mater. Res. **37**, 589 (2007).

[3] S. Park, P. Ryan, E. Karapetrova, J. W. Kim, J. X. Ma, J. Shi, J. W. Freeland, and W. Wu, Appl. Phys. Lett. **95**, 072508 (2009).

[4] J. Cao and J. Wu, Mater. Sci. Eng. R Reports **71**, 35 (2011).

[5] C. Becher, L. Maurel, U. Aschauer, M. Lilienblum, C. Magén, D. Meier, E. Langenberg, M. Trassin, J. Blasco, I. P. Krug, P. A. Algarabel, N. A. Spaldin, J. A. Pardo, and M. Fiebig, Nat. Nanotechnol. **10**, 661 (2015).

[6] Y. Maeno, T. M. Rice, and M. Sigrist, Phys. Today **54**, 42 (2001).

[7] S. Jin, M. McCormack, T. H. Tiefel, and R. Ramesh, J. Appl. Phys. **76**, 6929 (1994).

[8] J.-H. Park, E. Vescovo, H.-J. Kim, C. Kwon, R. Ramesh, and T. Venkatesan, Nature **392**, 794 (1998).

[9] A. I. Buzdin, J. Phys. Condens. Matter **11**, 1089 (1999).

[10] F. S. Bergeret, A. F. Volkov, and K. B. Efetov, **77**, 1321 (2005).

[11] M. Eschrig and T. Löfwander, Nat. Phys. **4**, 138 (2008).

[12] J. W. A. Robinson, J. D. S. Witt, and M. G. Blamire, Science (80-.). **329**, (2010).

[13] J. Linder and J. W. A. Robinson, Nat. Phys. **11**, 307 (2015).

[14] M. Eschrig, Reports Prog. Phys. **78**, 104501 (2015).

[15] M. S. Anwar, S. R. Lee, R. Ishiguro, Y. Sugimoto, Y. Tano, S. J. Kang, Y. J. Shin, S. Yonezawa, D. Manske, H. Takayanagi, T. W. Noh, and Y. Maeno, Nat. Commun. **7**, 1 (2016).

[16] P. M. R. Brydon and D. Manske, Phys. Rev. Lett. **103**, 1 (2009).

[17] Q. Cheng and B. Jin, Phys. B Condens. Matter **426**, 40 (2013).

[18] Z. Q. Mao, Y. Maenoab, and H. Fukazawa, Mater. Res. Bull. **35**, 1813 (2000).

[19] R. Fittipaldi, A. Vecchione, S. Fusanobori, K. Takizawa, H. Yaguchi, J. Hooper, R. S. Perry, and Y. Maeno, J. Cryst. Growth **282**, 152 (2005).

[20] R. Matzdorf, Z. Fang, Ismail, J. Zhang, T. Kimura, Y. Tokura, K. Terakura, and E. W. Plummer, Science **289**, 746 (2000).

[21] V. I. Nefedov and O. A. Baschenko, J. Electron Spectros. Relat. Phenomena **47**, 1 (1988).

[22] R. Bertacco, J. P. Contour, A. Barthélemy, and J. Olivier, Surf. Sci. **511**, 366 (2002).

[23] R. Herger, P. R. Willmott, C. M. Schlepütz, M. Björck, S. A. Pauli, D. Martoccia, B. D. Patterson, D. Kumah, R. Clarke, Y. Yacoby, and M. Döbeli, Phys. Rev. B - Condens. Matter Mater. Phys. **77**, 1 (2008).

[24] H. Dulli, P. A. Dowben, S. H. Liou, and E. W. Plummer, Phys. Rev. B - Condens. Matter Mater. Phys. **62**, R14629 (2000).

[25] T. T. Fister, D. D. Fong, J. A. Eastman, P. M. Baldo, M. J. Highland, P. H. Fuoss, K. R. Balasubramaniam, J. C. Meador, and P. A. Salvador, Appl. Phys. Lett. **93**, 151904 (2008).

[26] Z. Liao, F. Li, P. Gao, L. Li, J. Guo, X. Pan, R. Jin, E. W. Plummer, and J. Zhang, Phys.

Rev. B - Condens. Matter Mater. Phys. **92**, 1 (2015).

[27] C. Zener, Phys. Rev. **82**, 403 (1951).

[28] P. W. Anderson and H. Hasegawa, Phys. Rev. **100**, 675 (1955).

[29] L. Zhong Zhao and V. Young, J. Electron Spectros. Relat. Phenomena **34**, 45 (1984).

[30] H. Kurata and C. Colliex, Phys. Rev. B **48**, 2102 (1993).

[31] M. Varela, M. P. Oxley, W. Luo, J. Tao, M. Watanabe, A. R. Lupini, S. T. Pantelides, and S. J. Pennycook, Phys. Rev. B - Condens. Matter Mater. Phys. **79**, 1 (2009).

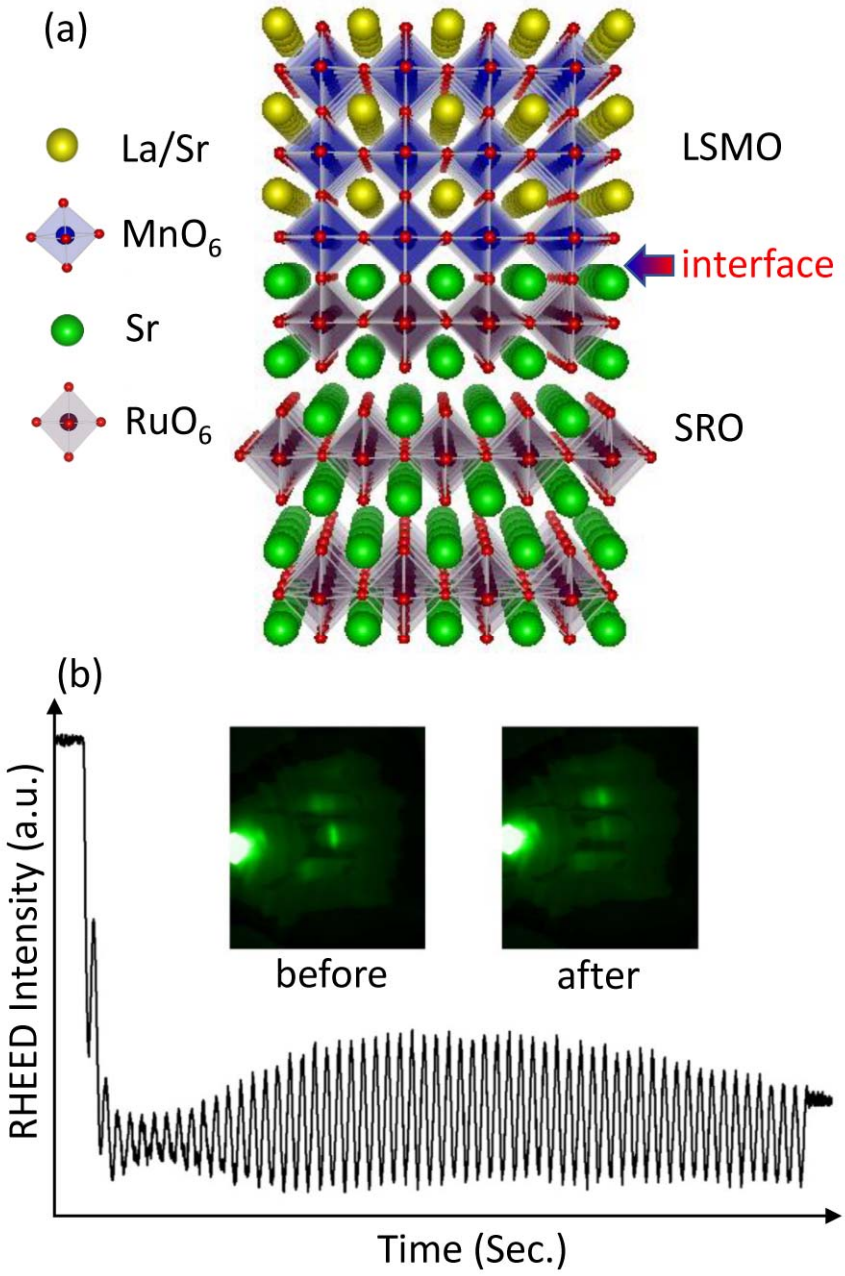

Figure 1. (a) A ball model showing the possible structure of growth of LSMO thin films on SRO214 single crystals. (b) The RHEED pattern before and after growth are sharp. The oscillations indicate layer-by-layer growth.

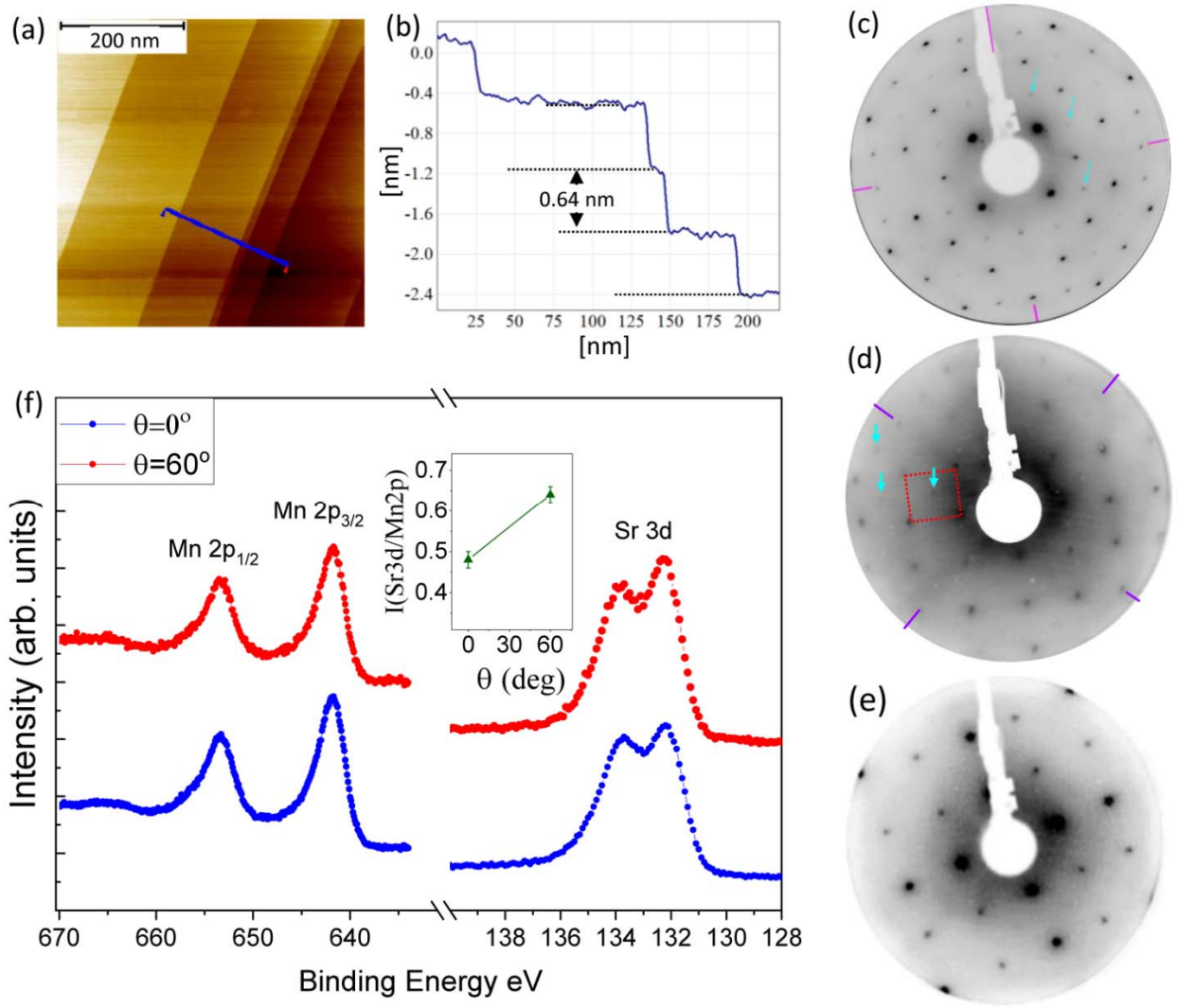

Figure 2. (a) STM topography image showing steps with flat terraces. (b) Line profile showing step heights. (c) LEED pattern of an as-cleaved SRO214 surface taken at room temperature showing fractional spots (indicated by arrows). There are no fractional spots along glide lines as indicated with solid lines. Electron energy of 195 eV was used. (d) A LEED surface structure of a substrate surface after annealing at 700 °C and 80 mTorr oxygen partial pressure. The primary (1×1) surface unit cell is marked by red square. (e) A LEED pattern of the 10 u.c. LSMO grown on SRO214 taken with electron energy of 107 eV showing no evident reconstruction. (f) XPS spectra of 10 unit-cell LSMO film taken at different emission angles θ in the region of Mn 2p and Sr 3d. The inset shows the ratio of intensity of Sr-3d peaks to Mn-2p as a function of collection angle.

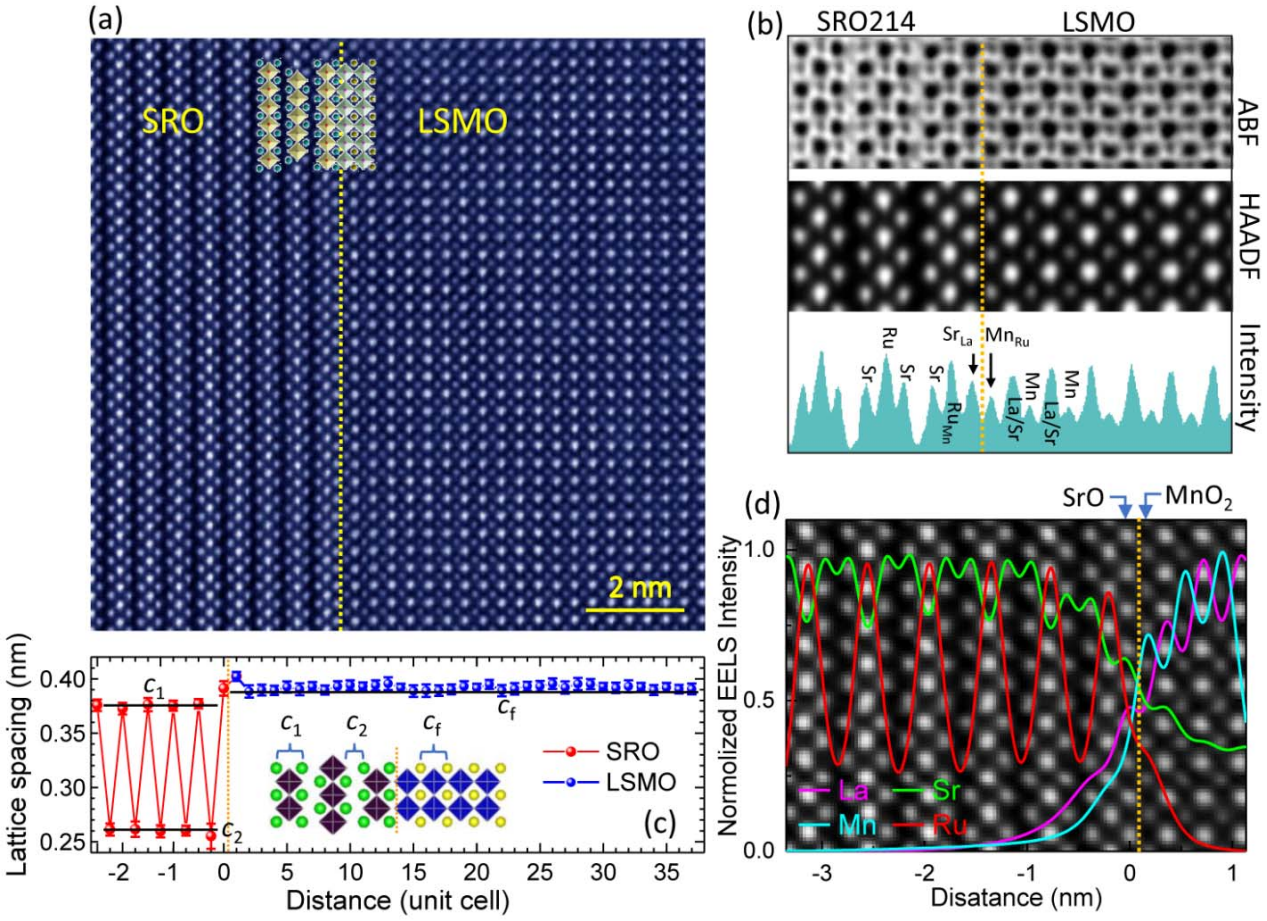

Figure 3. (a) A HAADF-TEM image near the interface of 60 u.c. LSMO thin film grown on SRO214 (001) substrate. (b) The comparison of HAADF- and ABF-STEM images as well as the intensity profile for the HAADF image taken along [100] direction. (c) Lattice spacing variation across the interface (see the labeling in the inset). (d) Composition profile extracted from EELS spectrum for La, Sr, Mn and Ru across the LSMO/SRO214 interface, illustrating the Mn-Ru and La-Sr diffusion at the interface.

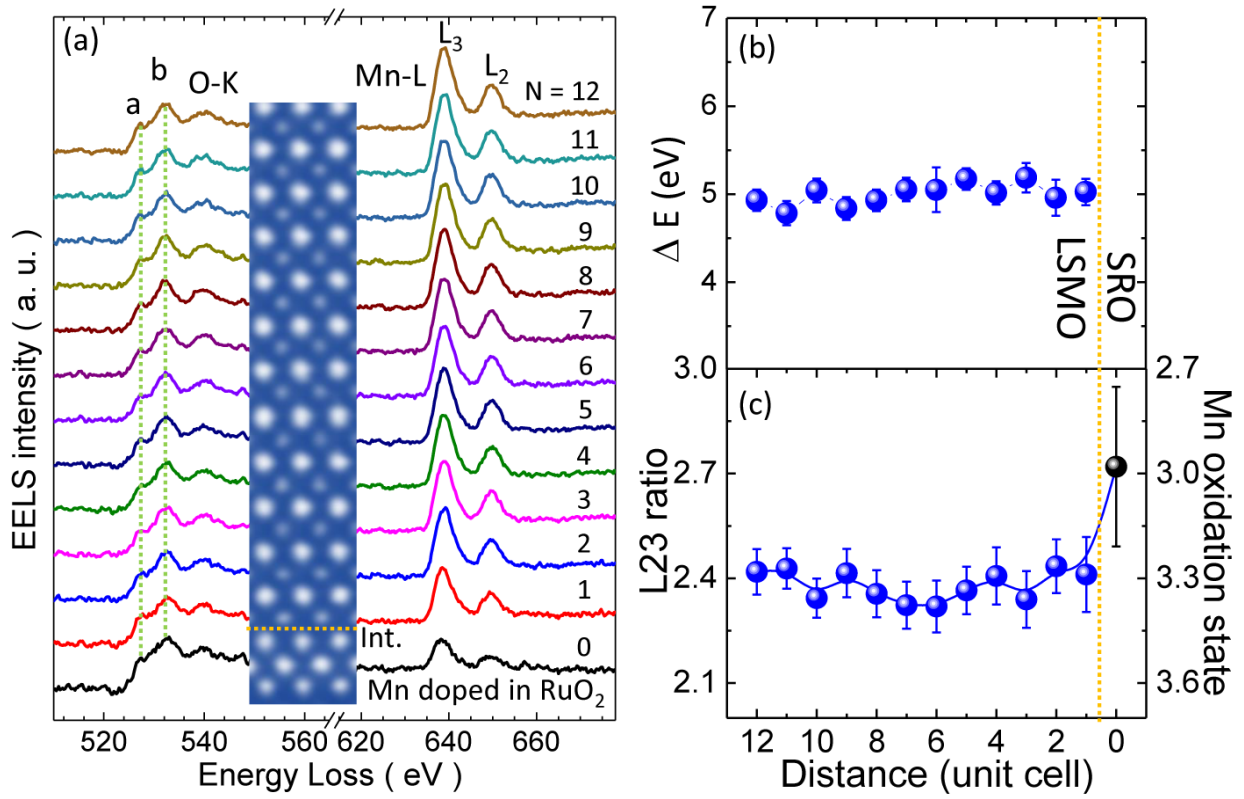

Figure 4. (a) Background subtracted EELS spectra of layer-by-layer O K edge and Mn L edge across the LSMO/SRO214 interface. The inset is the corresponding HAADF-STEM image. Evolution of Mn oxidation states determined by (b) energy separation (△E) between pre-peak (marked as a) and main peak (marked as b) in O-K edges and (c) L_{23} ratio (i.e., the intensity ratio of L_2 to L_3 peak) as a function of distance from interface. The dotted yellow line indicates the position of interface.